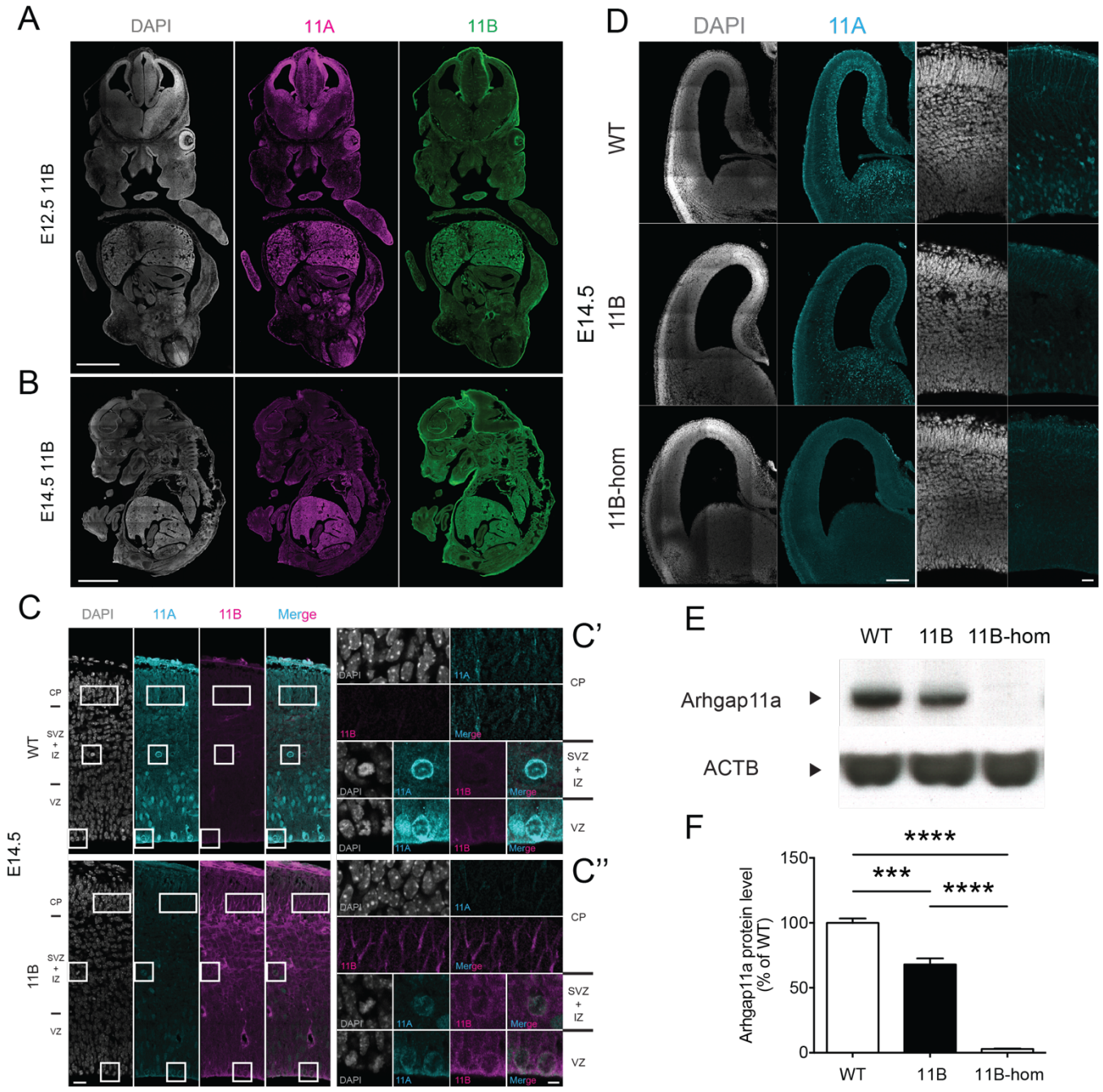


Appendix

Expression of human-specific ARHGAP11B in mice leads to neocortex expansion and increased memory flexibility

Lei Xing¹, Agnieszka Kubik-Zahorodna², Takashi Namba¹, Anneline Pinson¹, Marta Florio^{1†}, Jan Prochazka², Mihail Sarov¹, Radislav Sedlacek², Wieland B. Huttner^{1*}

Appendix Figure S1 - Expression of ARHGAP11B and decreased level of Arhgap11a in 11B mouse neocortex.	3
Appendix Figure S2 - Decreased level of Arhgap11a does not affect basal mitoses and BP abundance.	5
Appendix Figure S3 - Increased BP abundance in 11B mouse neocortex is not due to increased BP generation from APs nor to reduced BP apoptosis.	7
Appendix Figure S4 - Cell density in different cortical layers of mouse neocortex at E18.5 and P56, and abundance of glial cells and progenitors in embryonic 11B mice at E18.5.	9
Appendix Figure S5 - Adult hippocampal neurogenesis is not changed in 11B mice.	10
Appendix Figure S6 - Increased deep-layer neuron apoptosis in postnatal 11B mouse neocortex.	12
Appendix Figure S7 - 11B overexpression in electroporated mouse neocortex induces cortical folding and increases upper-layer neuron abundance.	13
Appendix Table S1 - Primers used for genotyping and qPCR analysis.	14



Appendix Figure S1 - Expression of ARHGAP11B and decreased level of Arhgap11a in 11B mouse neocortex.

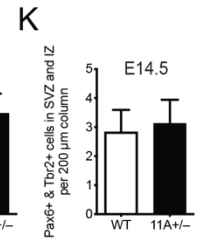
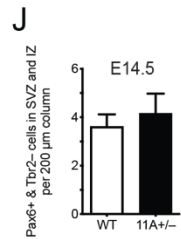
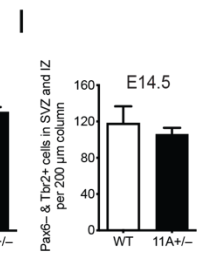
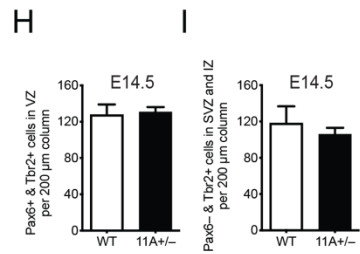
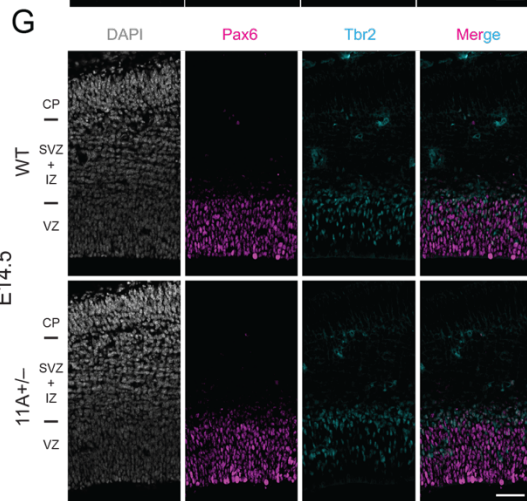
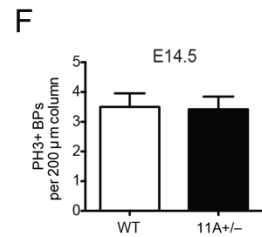
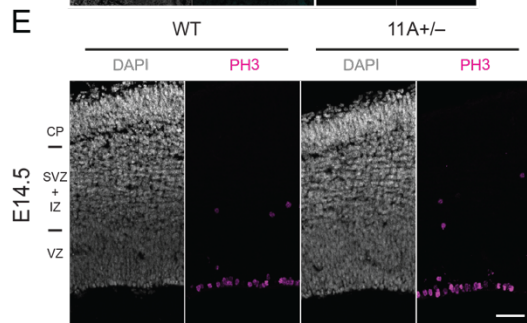
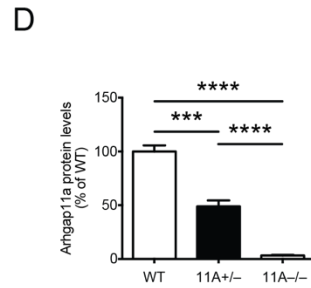
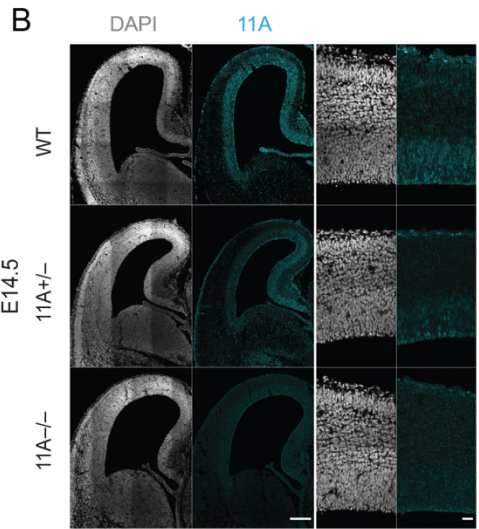
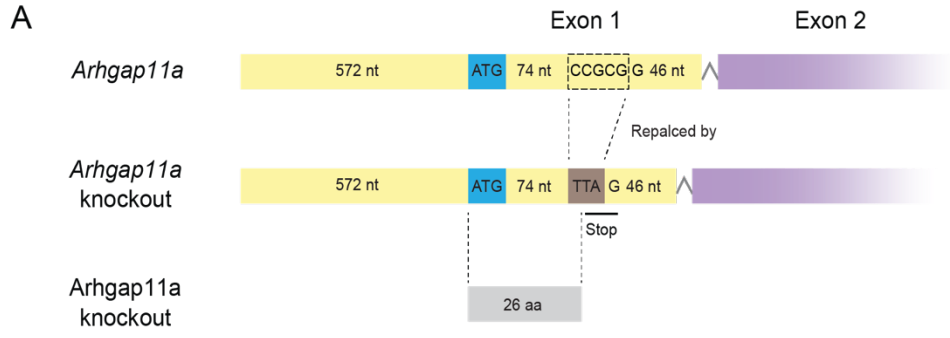
A, B Representative immunofluorescence for Arhgap11a (11A, magenta) and ARHGAP11B (11B, green), combined with DAPI staining (white), of E12.5 (A) and E14.5 (B) 11B mouse embryos. Images are single optical sections. Scale bars, 1000 μm (A); 2000 μm (B).

C Representative immunofluorescence for Arhgap11a (11A, cyan) and ARHGAP11B (11B, magenta), combined with DAPI staining (white), of E14.5 wildtype (WT) and 11B mouse dorsolateral neocortex rostrally. Boxes (50 μm x 25 μm and 25 μm x 25 μm) in (A) indicate areas in WT and 11B mouse neocortex that are shown at higher magnification in (A') and (A''), respectively. Images are single optical sections. Scale bars, 20 μm (A); 5 μm (A', A'').

D Representative immunofluorescence for Arhgap11a (11A, cyan), combined with DAPI staining (white), of E14.5 WT, heterozygous 11B (11B) and homozygous 11B (11B-hom) mouse dorsolateral neocortex rostrally. Images on the right show higher magnifications. Images are single optical sections. Scale bars, 200 μm (D, left); 30 μm (D, right).

E Representative immunoblots, using Arhgap11a and β -actin (ACTB) antibodies, of E14.5 WT, heterozygous 11B (11B) and homozygous 11B (11B-hom) mouse neocortex.

F Quantification of the ratio of Arhgap11a to β -actin of E14.5 WT, heterozygous 11B (11B) and homozygous 11B (11B-hom) mouse neocortex, using immunoblots obtained as in (E). Data are the mean of 3 (WT), 6 (11B) and 5 (11B-hom) embryos, which were derived from 3 separate litters. The WT mean was set to 100, and the other mean values are expressed relative to this. Note that there was no Arhgap11a detected in the 11B-hom mouse neocortex. Error bars indicate SD, one-way ANOVA followed by Tukey's multiple comparisons tests, *** $P < 0.001$, **** $P < 0.0001$. WT vs. 11B, $P = 0.0004$; WT vs. 11B-hom, $P < 0.0001$; 11B vs. 11B-hom, $P < 0.0001$



Appendix Figure S2 - Decreased level of Arhgap11a does not affect basal mitoses and BP abundance.

A Diagram showing the strategy of generating *Arhgap11a* knockout mice.

B Representative immunofluorescence for Arhgap11a (cyan), combined with DAPI staining (white), of E14.5 wildtype (WT), heterozygous *Arhgap11a* knockout (11A^{+/-}) and homozygous *Arhgap11a* knockout (11A^{-/-}) mouse dorsolateral neocortex rostrally. Images on the right show higher magnifications. Images are single optical sections. Scale bars, 200 μ m (left); 30 μ m (right).

C Representative immunoblots, using Arhgap11a and β -actin (ACTB) antibodies, of E14.5 WT, 11A^{+/-} and 11A^{-/-} mouse neocortex.

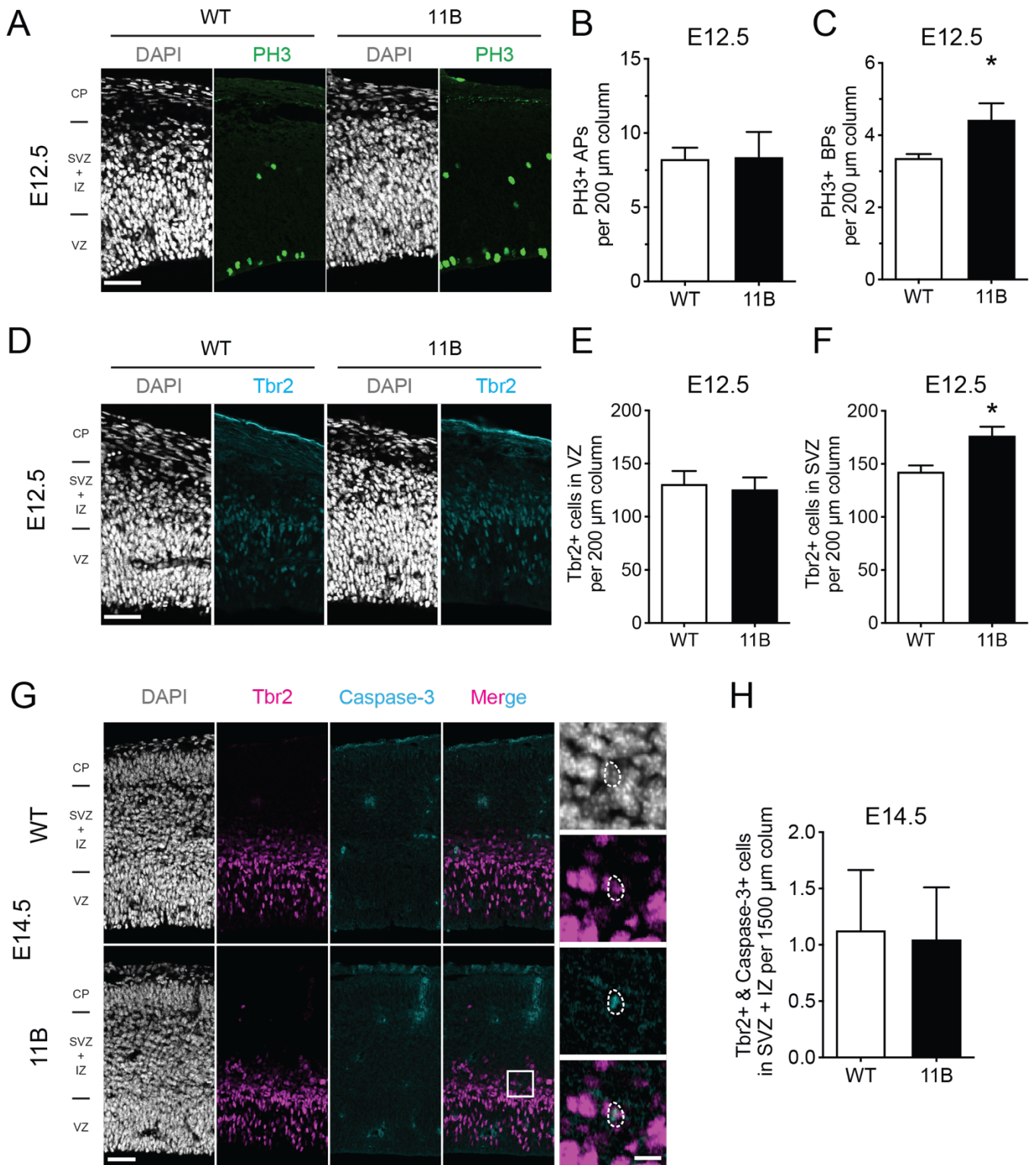
D Quantification of the ratio of Arhgap11a to β -actin of E14.5 WT, 11A^{+/-} and 11A^{-/-} mouse neocortex, using immunoblots obtained as in (C). Data are the mean of 4 (WT), 5 (11A^{+/-}) and 3 (11A^{-/-}) embryos, which were derived from 3 separate litters. The WT mean was set to 100, and the other mean values are expressed relative to this. Note that there was no Arhgap11a detected in the 11B-hom mouse neocortex. Error bars indicate SD, one-way ANOVA followed by Tukey's multiple comparisons tests, *** $P < 0.001$, **** $P < 0.0001$. WT vs. 11A^{+/-}, $P = 0.0001$; WT vs. 11A^{-/-}, $P < 0.0001$; 11A^{+/-} vs. 11A^{-/-}, $P = 0.0006$.

E Representative immunofluorescence for PH3 (magenta), combined with DAPI staining (white), of E14.5 WT and 11A^{+/-} mouse dorsolateral neocortex rostrally. Images are single optical sections. Scale bar, 50 μ m.

F Quantification of PH3⁺ mitotic BPs in a 200 μ m-wide column of E14.5 WT (white) and 11A^{+/-} (black) mouse neocortex, using immunostained cryosections obtained as in (E). Data are the mean of 6 (WT) and 7 (11A^{+/-}) embryos, which were derived from 3 separate litters. Error bars indicate SD, two-tailed unpaired Student's *t*-test.

G Representative immunofluorescence for Pax6 (magenta) and Tbr2 (cyan), combined with DAPI staining (white), of E14.5 WT and 11A^{+/-} mouse dorsolateral neocortex rostrally. Images are single optical sections. Scale bar, 50 μ m.

H-K Quantification of Pax6⁺/Tbr2⁺ cells in VZ (H), Pax6⁻/Tbr2⁺ cells in SVZ and IZ (I), Pax6⁺/Tbr2⁻ cells in SVZ and IZ (J) and Pax6⁺/Tbr2⁺ cells in SVZ and IZ (K) in a 200 μ m-wide column of E14.5 WT (white) and 11A^{+/-} (black) mouse dorsolateral neocortex rostrally, using immunostained cryosections obtained as in (G). Data are the mean of 6 (WT) and 7 (11A^{+/-}) embryos, which were derived from 3 separate litters. Error bars indicate SD, two-tailed unpaired Student's *t*-test.



Appendix Figure S3 - Increased BP abundance in 11B mouse neocortex is not due to increased BP generation from APs nor to reduced BP apoptosis.

A Representative immunofluorescence for PH3 (green), combined with DAPI staining (white), of E12.5 wildtype (WT) and 11B mouse dorsolateral neocortex rostrally. Images are single optical sections. Scale bars, 50 μm .

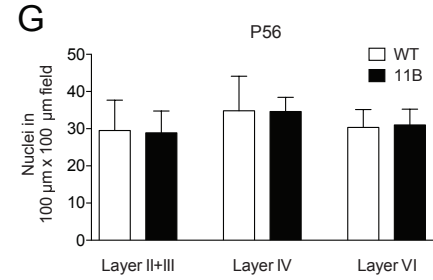
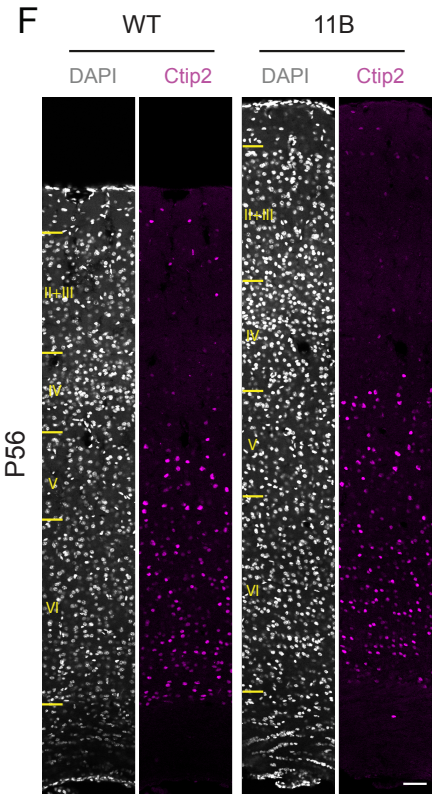
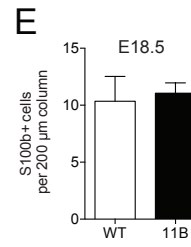
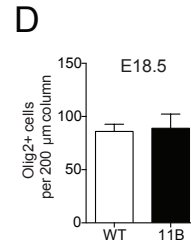
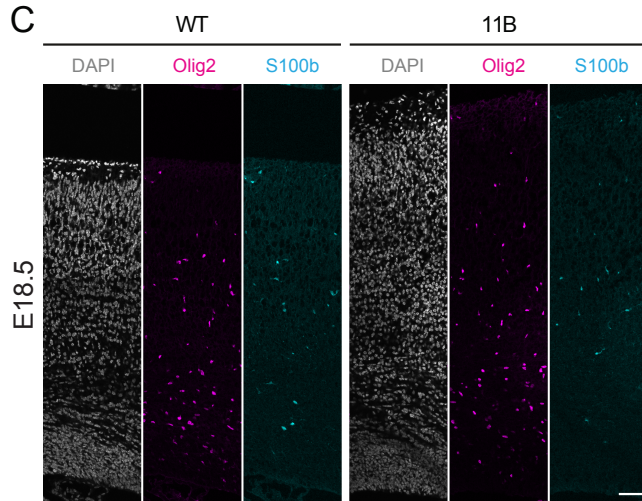
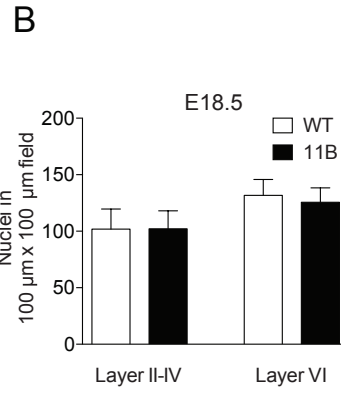
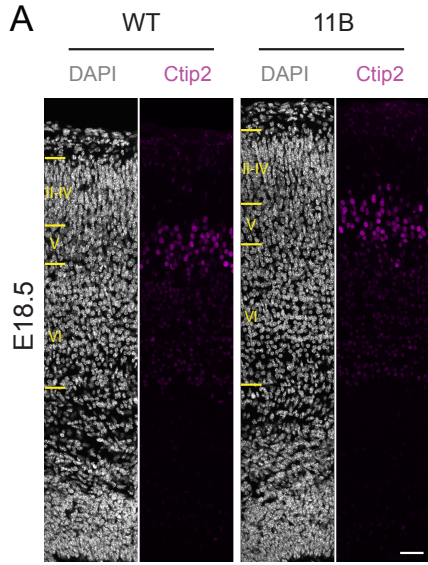
B, C Quantification of PH3⁺ APs (B) and PH3⁺ BPs (C) in a 200 μm -wide field of E12.5 WT (white) and 11B (black) mouse dorsolateral neocortex rostrally, using immunostained cryosections obtained as in (A). Error bars indicate SD, two-tailed unpaired Student's *t*-test, * $P = 0.0441$.

D Representative immunofluorescence for Tbr2 (cyan), combined with DAPI staining (white), of E12.5 WT and 11B mouse dorsolateral neocortex rostrally. Images are single optical sections. Scale bars, 50 μm .

E, F Quantification of Tbr2⁺ cells in VZ (E) and Tbr2⁺ cells in SVZ (F) in a 200 μm -wide field of E12.5 WT (white) and 11B (black) mouse dorsolateral neocortex rostrally, using immunostained cryosections obtained as in (D). Error bars indicate SD, two-tailed unpaired Student's *t*-test, * $P < 0.05$. $P = 0.0272$ (F).

G Representative immunofluorescence for Tbr2 (magenta) and active caspase-3 (cyan), combined with DAPI staining (white), of E14.5 wildtype (WT) and 11B mouse dorsolateral neocortex rostrally. Images are single optical sections. Scale bars, 50 μm (left); 10 μm (right).

H Quantification of Tbr2⁺ & active caspase-3⁺ cells in SVZ in a 1500 μm -wide column of E14.5 WT (white) and 11B (black) mouse neocortex, using immunostained cryosections obtained as in (G). Data are the mean of 9 (WT) and 12 (11B) embryos, which were derived from 3 separate litters. Error bars indicate SD, two-tailed unpaired Student's *t*-test.



Appendix Figure S4 - Cell density in different cortical layers of mouse neocortex at E18.5 and P56, and abundance of glial cells and progenitors in embryonic 11B mice at E18.5.

A Representative immunofluorescence for Ctip2 (magenta), combined with DAPI staining (white), of E18.5 wildtype (WT) and 11B mouse neocortex at the position where cortical thickness was measured (Fig 2A, red lines). Yellow lines indicate boundaries between different cortical layers, which are defined based on Ctip2 staining. Images are single optical sections. Scale bar, 50 μm .

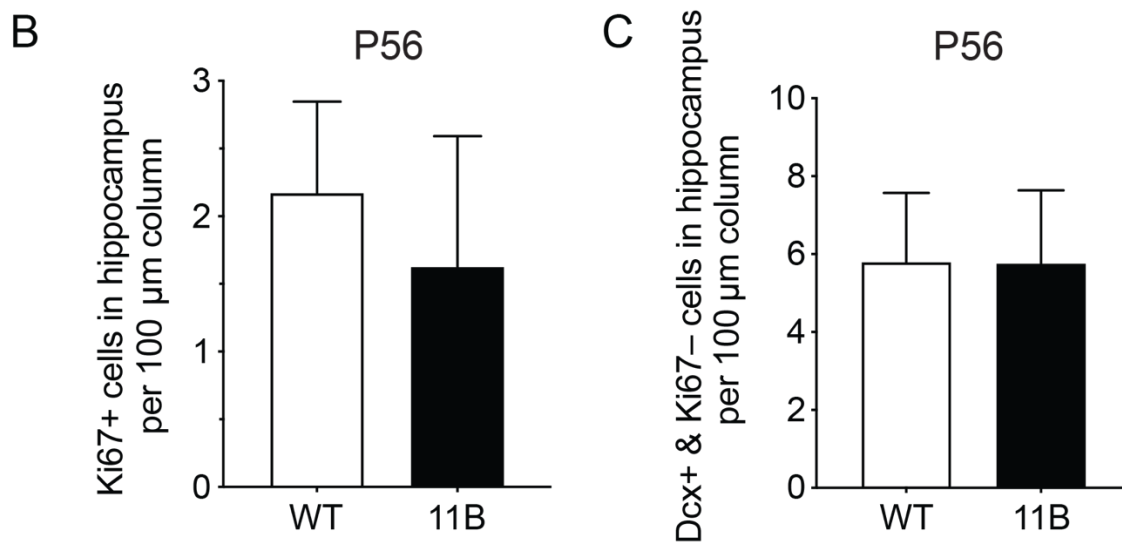
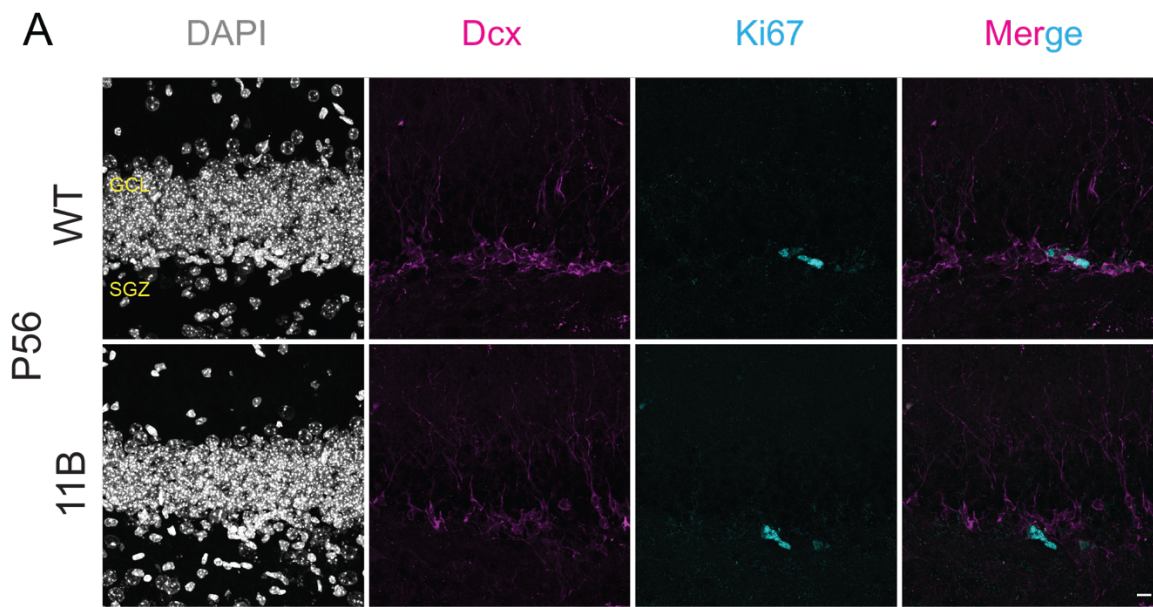
B Quantification of cell density in different cortical layers of E18.5 WT (white) and 11B (black) mouse neocortex at the position where cortical thickness was measured (Fig 2A, red lines), using immunostained cryosections obtained as in (A). Data are the mean of 6 (WT) and 12 (11B) embryos, which were derived from 3 separate litters. Error bars indicate SD, two-tailed unpaired Student's *t*-test.

C Representative immunofluorescence for Olig2 (magenta) and S100b (cyan), combined with DAPI staining (white), of E18.5 WT and 11B mouse neocortex at the position where cortical thickness was measured (Fig 2A, red lines). Images are single optical sections. Scale bar, 50 μm .

D, E Quantification of Olig2+ (D) and S100b+ (E) cells in a 200 μm -wide column of E18.5 WT (white) and 11B (black) mouse neocortex, using immunostained cryosections obtained as in (C). Data are the mean of 3 (WT) and 4 (11B) embryos, which were derived from 3 separate litters. Error bars indicate SD, two-tailed unpaired Student's *t*-test.

F Representative immunofluorescence for Ctip2 (magenta), combined with DAPI staining (white), of P56 adult WT and 11B mouse neocortex at the position where cortical thickness was measured (Fig 3D, red lines). Yellow lines indicate boundaries between different cortical layers, which are defined based on Ctip2 staining. Images are single optical sections. Scale bar, 50 μm .

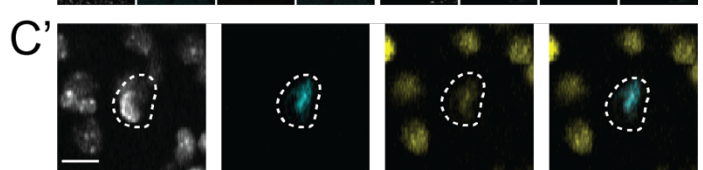
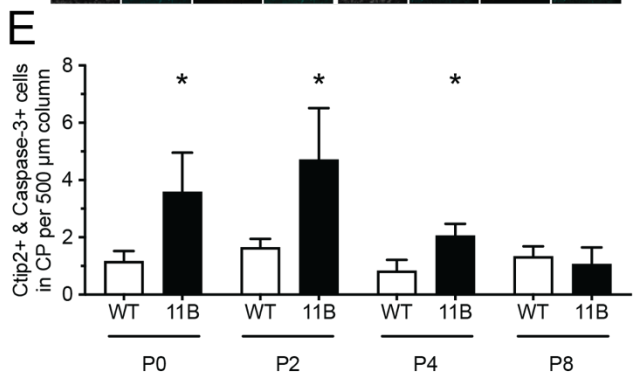
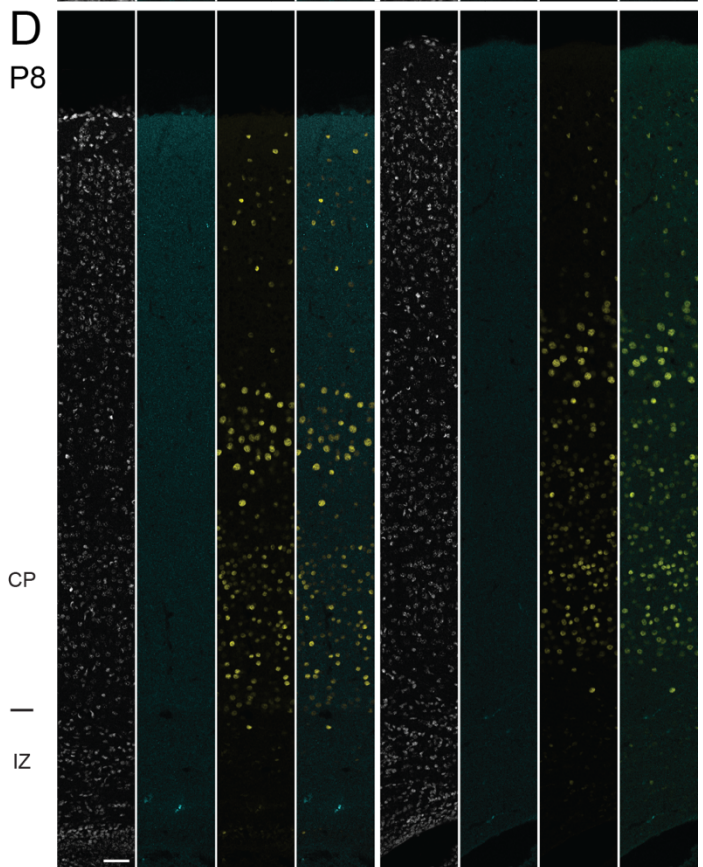
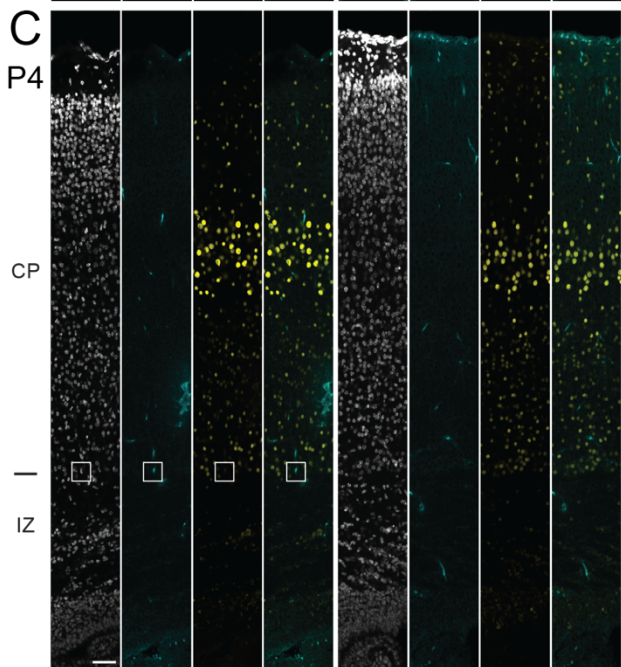
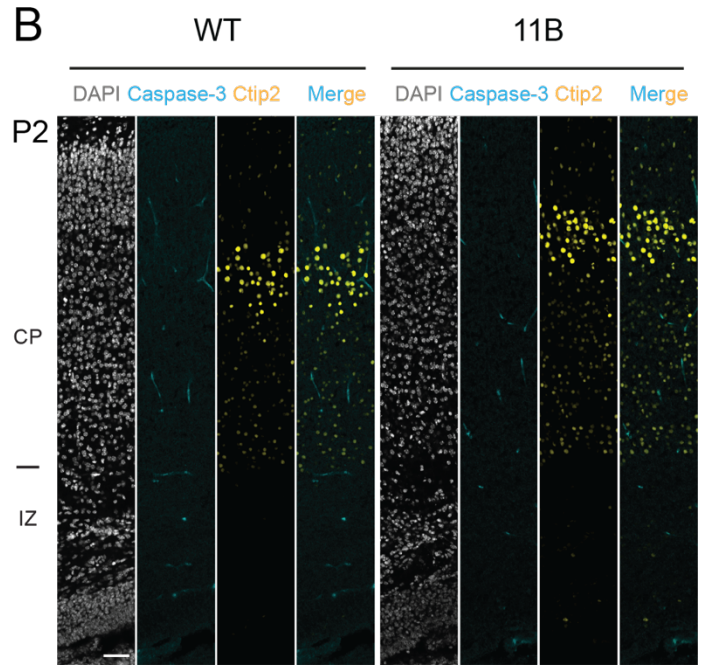
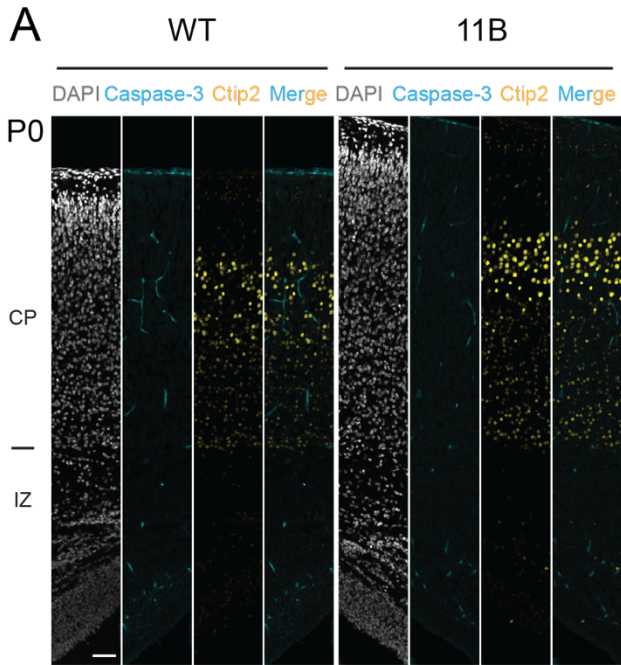
G Quantification of cell density in different cortical layers of P56 adult WT (white) and 11B (black) mouse neocortex at the position where cortical thickness was measured (Fig 3D, red lines), using immunostained cryosections obtained as in (F). Data are the mean of 6 (WT, 3 male; 3 female) and 8 (11B, 4 male; 4 female) adult mice. Error bars indicate SD, two-tailed unpaired Student's *t*-test.



Appendix Figure S5- Adult hippocampal neurogenesis is not changed in 11B mice.

A Representative immunofluorescence for doublecortin (Dcx, magenta) and Ki67 (cyan), combined with DAPI staining (white), of adult wildtype (WT) and 11B mouse hippocampus at P56. Images are maximum intensity projection of three optical sections. Scale bar, 10 μm.

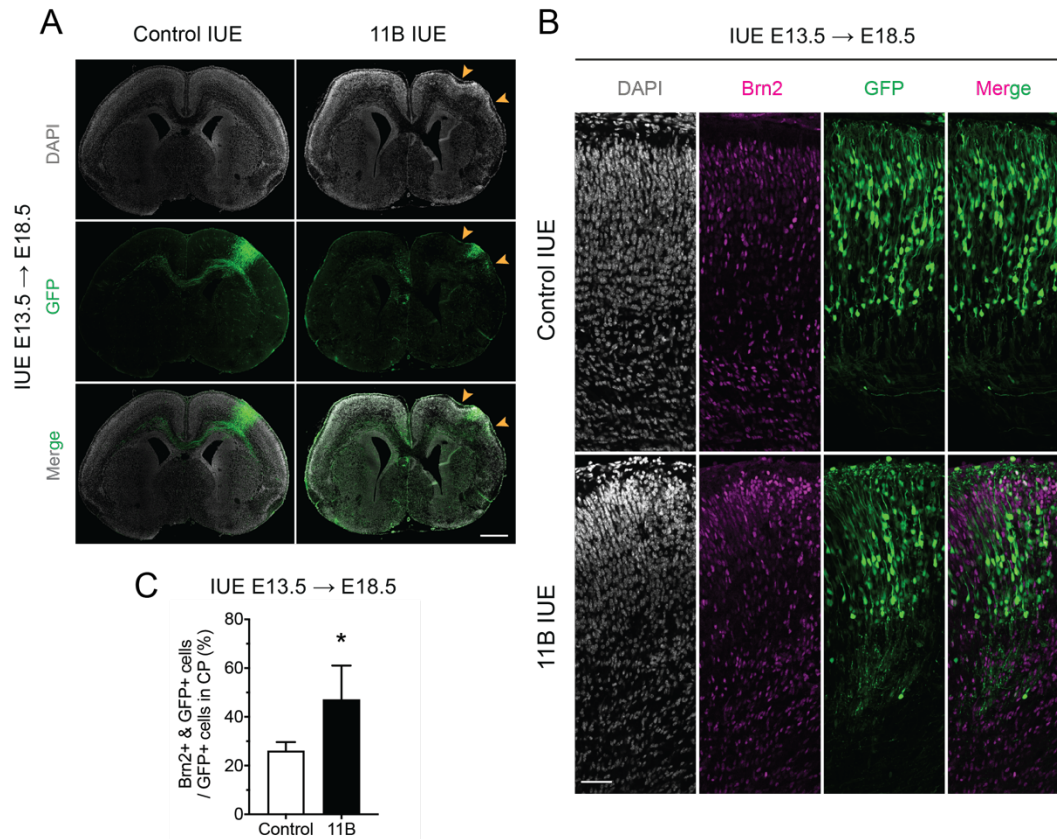
B, C Quantification of the abundance of Ki67+ cells (B, NPCs) and Dcx+ & Ki67- cells (C, newborn neurons) in a 100 μm-wide column of adult WT (white) and 11B (black) mouse hippocampus, using immunostained cryosections obtained as in (A). Data are the mean of 7 (WT, 3 male; 4 female) and 8 (11B, 4 male; 4 female) mice. Error bars indicate SD, two-tailed unpaired Student's *t*-test.



Appendix Figure S6 - Increased deep-layer neuron apoptosis in postnatal 11B mouse neocortex.

A-D Representative immunofluorescence for active caspase-3 (cyan) and Ctip2 (yellow), combined with DAPI staining (white), of P0 (A), P2 (B), P4 (C) and P8 (D) wildtype (WT) and 11B mouse dorsolateral neocortex rostrally. Boxes (40 μm x 45 μm) in (C) indicate areas in WT mouse neocortex that are shown at higher magnification in (C'). Images are single optical sections. Scale bars, 50 μm (A-D); 10 μm (C').

E Quantification of Ctip2+ & active caspase-3+ cells in the CP in a 500 μm -wide column of postnatal WT (white) and 11B (black) mouse neocortex, using immunostained cryosections obtained as in (A-D). Data are the mean of 3-9 (WT) and 4-6 (11B) pups at each stage analysed, which were derived from 3 separate litters. Error bars indicate SD, two-tailed unpaired Student's *t*-test, * $P < 0.05$. $P = 0.0429$ (P0); $P = 0.0291$ (P2); $P = 0.0484$ (P4).



Appendix Figure S7 - 11B overexpression in electroporated mouse neocortex induces cortical folding and increases upper-layer neuron abundance.

E13.5 wildtype mouse neocortex were subjected to IUE with a plasmid encoding GFP, together with either an empty plasmid or a plasmid encoding *ARHGAP11B*, followed by analysis at E18.5.

A Representative immunofluorescence for GFP (green), combined with DAPI staining (white), of control and *ARHGAP11B*-electroporated mouse dorsolateral neocortex rostrally. Note the neocortex folding induced by *ARHGAP11B* overexpression, as indicated by the yellow notched arrowheads. Images are single optical sections. Scale bars, 500 μ m.

B Representative immunofluorescence for Brn2 (magenta) and GFP (green), combined with DAPI staining (white), of the targeted area of control (unfolded) and *ARHGAP11B*-electroporated (folded) mouse dorsolateral neocortex rostrally. Images are single optical sections. Scale bars, 50 μ m.

C Quantification of the percentage of GFP+ cells in the CP of the targeted area of neocortex that are Brn2+, upon control (white) and *ARHGAP11B* (black) electroporation, using immunostained cryosections obtained as in (B). Data are the mean of 4-5 embryos, which were derived from four separate litters. Error bars indicate SD; * $P = 0.0225$.

Appendix Table S1 - Primers used for genotyping and qPCR analysis.

Primers for genotyping			
11B mouse line	Forward	5'-ATGGACAGCAGCAATCTTGC	
	Reverse	5'-TTTCCTTTCCCATGCCAGAG	
Arhgap11a knock out mouse line	Forward	5'-GCAAGTGGAAGAGTTGGTTG	
	Reverse	5'-AAAACCCACGGCAACATAGG	
Primers for qPCR			
Human	<i>ARHGAP11B</i>	Forward	5'-GGAGTAGCACAGAGA
		Reverse	5'-TGAGAATAAGATGGATAGCAGCA
	<i>ARHGAP11A</i>	Forward	5'-AGCAGTTCTACACCGGTATCA
		Reverse	5'-ACCTGCAGTGATCAAATGGT
	<i>GAPDH</i>	Forward	5'-AAGGTGAAGGTCGGAGTCAA
		Reverse	5'-AATGAAGGGGTCATTGATGG
Mouse	<i>mARHGAP11B</i>	Forward	5'-GGAGTAGCACAGAGA
		Reverse	5'-TGAGAATAAAAATGGACAGCAGCA
	<i>Arhgap11a</i>	Forward	5'-TCCGTCAGTCCGTCAGAAGA
		Reverse	5'-CTGCGTCACCAAAGATTGCC
	<i>Gapdh</i>	Forward	5'-TGAAGCAGGCATCTGAGGG
		Reverse	5'-CGAAGGTGGAAGAGTGGGAG